

Airborne characterization of the Andasol 3 solar field

Christoph Prah, Laura Porcel, Marc Röger, and Niels Algner

Citation: [AIP Conference Proceedings](#) **2033**, 030013 (2018); doi: 10.1063/1.5067029

View online: <https://doi.org/10.1063/1.5067029>

View Table of Contents: <http://aip.scitation.org/toc/apc/2033/1>

Published by the [American Institute of Physics](#)

Articles you may be interested in

[Identification of optimum molten salts for use as heat transfer fluids in parabolic trough CSP plants. A techno-economic comparative optimization](#)

[AIP Conference Proceedings](#) **2033**, 030012 (2018); 10.1063/1.5067028

[Deploying enclosed trough for thermal EOR at commercial scale](#)

[AIP Conference Proceedings](#) **2033**, 030002 (2018); 10.1063/1.5067018

[MicroSol-R: Versatile solar facility for research and industry](#)

[AIP Conference Proceedings](#) **2033**, 030003 (2018); 10.1063/1.5067019

[The design of dust barriers to reduce collector mirror soiling in CSP plants](#)

[AIP Conference Proceedings](#) **2033**, 030017 (2018); 10.1063/1.5067033

[Design of a molten salt parabolic trough power plant with thermal energy storage and a novel freezing protection](#)

[AIP Conference Proceedings](#) **2033**, 030005 (2018); 10.1063/1.5067021

[Evaluation of the tracking accuracy of parabolic-trough collectors in a solar plant for district heating](#)

[AIP Conference Proceedings](#) **2033**, 030015 (2018); 10.1063/1.5067031

AIP | Conference Proceedings

Get **30% off** all
print proceedings!

Enter Promotion Code **PDF30** at checkout



Airborne Characterization of the Andasol 3 Solar Field

Christoph Prah1^{1, a)}, Laura Porcel^{2, b)}, Marc Röger¹ and Niels Algner¹

¹German Aerospace Center (DLR e.V.), Solar Research, PSA, 04200 Tabernas, Spain.

²Laura Porcel Sendrós, Marquesado Solar, Andasol 3 TS Power Plant, A-92 km. 312, 18514 (Aldeire-La Calahorra) Granada, Spain.

^{a)}Corresponding author: christoph.prahl@dlr.de

^{b)}lporcel@marquesadosolar.com

Abstract. The solar-thermal parabolic trough power plant Andasol 3 (AS3) near Granada/Spain operated by Marquesado Solar SL (MQS) was commissioned in autumn 2011. The installed capacity of 49.9 MW_{el} in combination with thermal energy storage (TES) capacity for 7.5 hours at full load results in a net annual energy production of more than 165 GWh¹ (Dinter and Gonzalez 2014). The German Aerospace Center (DLR) has developed a tool for airborne characterization of entire parabolic trough plants. The approach called QFly_{SURVEY} uses an unmanned aerial vehicle (UAV) equipped with a high resolution digital still camera and delivers effective mirror slope deviation and the absolute orientation of the optical axis of each solar collector element (SCE). In order to validate and demonstrate QFly_{SURVEY}, a comprehensive measurement campaign was undertaken in the AS3 power plant in cooperation with MQS between 2016-10-24 and 2016-11-14. The main objective was to demonstrate the advantages of airborne solar field characterization in terms of rapid data acquisition, negligible interference with plant operation, and without the need of any additional installation of measurement equipment in the solar field. QFly_{SURVEY} provides accurate quantitative measures of optical performance of the solar field and supports the maximization of the thermal energy collected from the solar field by identifying low performing areas and the causes for optical losses.

INTRODUCTION

Both newly erected and operational CSP plants using parabolic trough collectors (PTC) have a certain potential to optimize the thermal output of the solar field. In order to evaluate this potential for a representative parabolic trough plant, a comprehensive measurement campaign was undertaken in the Andasol 3 (AS3) power plant in cooperation with Marquesado Solar (MQS) between 2016-10-24 and 2016-11-14. It should be stated that the production figures of AS3 exceed the expectations, outperforming the final performance test (FPT) numbers by ~10% (Vauth, RWE et al. 2016). However, MQS has observed that one of the four blocks of the solar field shows slightly reduced thermal performance. So the objective of the described work was to find a reason for the observed performance variation, and to check whether there are additional possibilities for action to further boost the plant performance.

Efficient and comprehensive characterization of CSP concentrators are preferably implemented by optical measurement methods (Xiao, Wei et al. 2012). Combining these methods with unmanned aerial vehicles (UAVs) provides the necessary speed and flexibility of the data acquisition and helps to overcome limitations of state of the art ground based methods. The objective of former implementation of airborne characterization of PTCs was to derive high resolution slope deviations in curvature direction (SD_x) and lateral/vertical absorber tube deviation from the focal line $\Delta X_{Abs}/\Delta Z_{Abs}$ for smaller measurement volumes like single solar collector assemblies (SCAs). This measurement mode is denoted QFly_{HighRes} (Prah1, Stanicki et al. 2013). However, the QFly_{HighRes} is not applicable to entire solar field due to relatively complex flight routes and low flight altitude.

¹ 12% of the annual production has been produced by natural gas usage. With the change of Spanish regulations, this 12% share is not being used anymore

The QFly_{SURVEY} concept presented here provides effective mirror slope deviations ($SD_{X_{eff}}$) and absolute orientation of each SCE's optical axis (θ) at lower spatial resolution from images taken along straight east-west flyovers at flight altitudes higher than 100 m. QFly_{SURVEY} data acquisition for the complete characterization of a AS3 solar field (1.5 x 1.3 km²) can be implemented in four to eight flights with a total flight time of 1-2 hours. The QFly_{SURVEY} approach can be also applied to an operational solar field under full solar radiation and in tracking mode for characterization of the tracking system.

The first objective of the presented measurement campaign was to demonstrate that the data acquisition for airborne solar field characterization is completed within less than four hours while minimizing the interference with plant operation and without additional installation of measurement equipment in the solar field. As the presented campaign was the first implementation of the QFly_{SURVEY} approach, the results have been validated against the already proven QFly_{HighRes} methods. From the plant operator's point of view, the benefit of QFly_{SURVEY} is assessed by its capability to uncover yet unknown irregularities in the solar field and to estimate the potential for optimization. While any deviation of the collector structure offers few options for improvements, tracking and SCE alignment provides much room for optimization by adjusting SCE alignment or inclinometer off-sets, with remarkable impact on the optical performance. This article addresses the following items and tasks:

- Measurands and scope of the airborne measurement in the AS3 plant
- Hardware and software components
- Data evaluation and workflow
- Measurement accuracy
- Results on solar field performance and solar field status
- Potential for optimization

Scope of the Measurement

This article focusses on the characterization of the optical performance determined by the concentrator geometry and solar field status. The corresponding raw data consists of RGB images captured with an off-the-shelf optical camera. Thermographic cameras can detect irregularities in receiver and piping thermal losses. (Jorgensen, Burkholder et al. 2009). This topic will be addressed in future activities in AS3.

For the **solar field performance**, the following measurands are obtained by QFly_{SURVEY}:

- Effective mirror slope deviations ($SD_{X_{eff}}$): This quantity comprises all effects including mirror slope deviations (SD_X), absorber tube deviation from the focal line ($\Delta X_{Abs}/\Delta Z_{Abs}$), and relative misalignment of SCEs within a single SCA ($\Delta\theta$). All these parameters leave characteristic traces in $SD_{X_{eff}}$ -maps, but the individual contributions cannot be measured independently from each other.

The position of the absorber tube (which actually provides the reflection pattern) has a major impact on the result. For this reason, the assumptions on the yet unknown absorber position must be carefully selected. For the absorber deviation in x-direction ΔX_{Abs} , an optimal position is assumed ($\Delta X_{Abs} = 0$). For the large systematic values of ΔZ_{Abs} for lower HTF temperatures, the assumption of an ideal positioning ($\Delta Z_{Abs} = 0$) would lead to implausible results. To prevent that, a model describing ΔZ_{Abs} as a function of the support geometry and the HTF temperature was implemented, in order to avoid systematic effect of the HTF-temperature on the $SD_{X_{eff}}$. Possible deviations from the zenith orientation are compensated during the calculation of $SD_{X_{eff}}$ calculation by balancing the average $SD_{X_{eff}}$ values from both sides of the parabola.

- Effective tracking deviation ($\Delta\theta$) refers to the deviation of the orientation of the optical axis of each SCE, including effects of systematic lateral absorber tube deviation and slope deviations of the mirror surface. In other words, $\Delta\theta$ describes the orientation of the effective parabola optical axis including possible systematic lateral absorber tube deviations ΔX_{Abs} . This deviation refers to a given set point defined by the solar field control system. Deviations may be caused either by malfunction of the tracking system, SCE misalignment (due to assembly inaccuracy) or torsion (due to operational loads like friction, wind, and unbalance).

These two measurands are indispensable to estimate the intercept factor (γ) and thus to derive the optical performance under the assumption of a certain mirror reflectivity and absorber performance².

² Characterized by glass envelope tube transmissivity and absorber tube absorptivity

The **solar field status** describes the condition of components in the solar field, in the first place mirrors and absorber tubes (aka: heat collecting elements (HCEs)). QFly_{SURVEY} provides the status, exact location and statistics for broken or missing mirror panels and broken receiver glass envelope tubes.

In the course of the measurement campaign, airborne data acquisition was carried out for the entire AS3 solar field, but only two out of four blocks were evaluated. The reason is that three blocks showed similar thermal performance, while one block is characterized by a small but significant reduction of the thermal output compared to the rest of the solar field. **FIGURE 1** provides an overview on the measurement volume and flight route.

Data acquisition was performed in two different operation modes of the solar field:

- *Offline*: All SCAs were facing zenith ($\theta = 90^\circ$) before or after solar noon, so that there was no concentrated radiation on the absorber. This data was used to calculate SD_{Xeff} maps with a spatial resolution of 20 mm/pixel and individual tracking angle θ of each SCE.
- *Online*: All SCAs in tracking mode and with DNI > 500 W/m². Under these conditions, a new method to determine tracking deviation $\Delta\theta$ was tested.

In addition, four of the SCAs were measured also with high precision inclinometers and with the QFly_{HighRes} method in order to provide benchmark data for the validation of results obtained with QFly_{SURVEY}.

This article presents only *offline* results as this method delivers both SD_{Xeff} maps and the tracking angle θ of each SCE. The additional value of *online* evaluation lies in the possibility to check the tracking performance during operation and the ability to detect defective absorber tubes. However, these results are beyond the scope of this article.

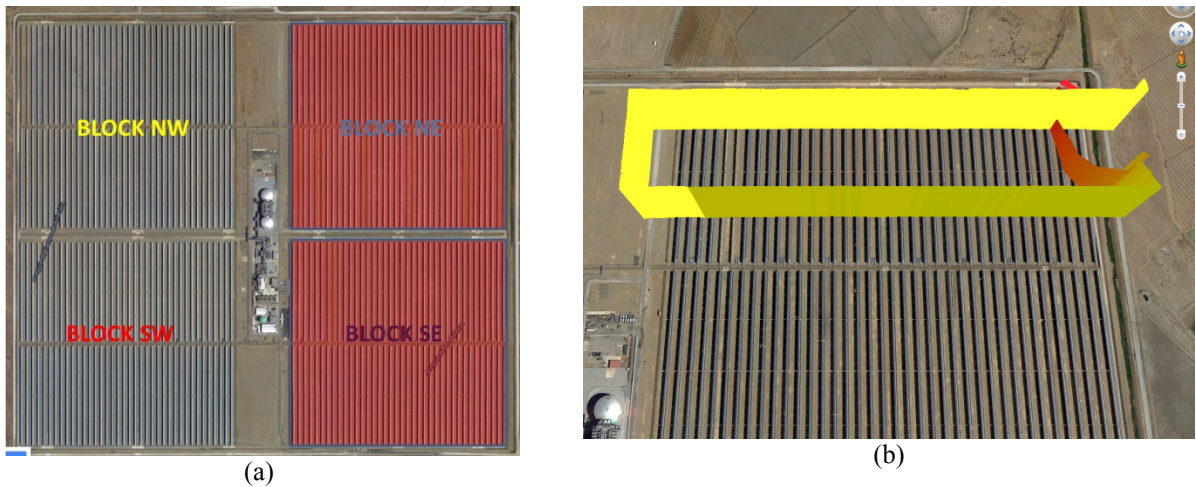


FIGURE 1. (a): Google Earth view with evaluated blocks North-East (NE) and South-East (SE). (b): Visualization of single flight route for the QFly_{SURVEY} data acquisition of a half block.

In order to identify the SCAs within the solar field, the “*YX-NN*” nomenclature is used in the following: Here, *Y* denotes the side of the solar field (e.g. L for left (west) and R for right (east)). The second letter *X* describes the position in North-South direction. Here, A-D refers to the southern blocks, and E-F to the northern block. Finally, the number *NN* describes the SCA position within the block from west to east, in the range of 01-38.

MEASUREMENT METHODOLOGY

The QFly System

The QFly system consists of off-the-shelf hardware and custom software for preparation and evaluation. The deployed UAV to carry the camera to the specified perspectives above the solar field is a microdrones md4-1000. It provides a flight time of up to 45 min, payload of up to 1.2 kg and autonomous waypoint navigation. The utilized recording device is a Sony NEX-7 camera with a 16 mm lens and 24 mega pixel resolution. The payload is

connected with a 2-axis gimbal to the UAV that enables pitch movement and compensates roll motions during flight.

The core of the QFly system is the software. Custom MATLAB code is used for the master program, including parameterized creation of the flight routes and the complete evaluation of the data. Additional software used for QFly are the AICON 3D studio (close range photogrammetry), mdCockpit (visualization of flight routes and data acquisition), SPRAY/STRAL (ray tracing), and GREENIUS (yield analysis).

There are two optical measurement methods employed by the QFly_{SURVEY} system:

1. Close range photogrammetry (PG): PG is used in the first place for camera calibration (determination of the inner orientation: IOR) and single image resection for camera orientation.
2. Deflectometry: The TARMES principle (Ulmer, Heinz et al. 2009) is used for the calculation of SD_{Xeff} maps. The images used for this purpose are also used for the calculation of the tracking angle θ based on a methodology presented by NREL (Jorgensen, Burkholder et al. 2009).

Flight Route Design and Solar field Status

The altitude for QFly_{SURVEY} data acquisition, if not limited by law/regulations, should allow for a visible length at ground level covering one loop in north-south direction of the solar field. With the currently used camera and flight route design, a flight altitude of 240 m above ground level would be required. Since UAV regulations in Spain restrict flight altitudes to 120 m above ground level, the effort is doubled to what is considered the optimum from a technical point of view. The trajectory is shown in **FIGURE 1**. The corresponding ground sample distance and thus spatial resolution of the SD_{Xeff} maps is about 30 mm/pixel (factor 5 below QFly_{HighRes}). In order to minimize flight altitude, the landscape camera orientation in north - south direction in combination with Nadir mount³ is applied. Future flight route designs will make use of different camera orientations (Oblique mode) and larger view angle in east-west direction for better pose estimation.

The requirements on the solar field status refer mainly to cleanliness, HTF temperature and tracking angle. Mirrors and absorber glass envelope tubes must be clean prior to the data acquisition. The tracking angle θ should be close to zenith for offline measurements. For online measurements, there are no θ -constraints. Constant HTF temperature and access to the plant data acquisition system is required in order to calculate the temperature dependent absorber tube position in vertical direction $\Delta Z_{Abs}(T_{HTF})$.

Concerning the ambient conditions, the wind speed at ground level must not exceed 6-8 m/s. Sufficient ambient light is required to keep exposure times as short as possible ($\leq 1/2000$ sec.) to avoid blurring.

Evaluation

The position and orientation of the camera (aka: EOR for “*exterior orientation*”) relative to the solar field is the key input parameter for all subsequent evaluation steps. Increasing flight altitude by a factor of five to ten with respect to the QFly_{HighRes} approach leads to the fact that PG based pose estimation used in QFly_{HighRes} cannot be deployed any more. The detection of single mirrors corners and artificial targets with reasonable dimensions is no longer possible from this altitude and flight routes with appropriate geometry would be far too long. It is therefore appropriate to assume a given field geometry and pre-calibration of the camera, and only to optimize the EOR by means of single photo resection (Grussenmeyer and Al Khalil 2002). 3D-object coordinates (inter SCA-gaps of the solar field) and IOR are provided as constraints, so that only the six parameters of the EOR are determined by optimization. The objective function of this optimization is the RMS-value of the residuals between detected⁴ and projected image coordinates. The uncertainty for the obtained EOR parameters has been estimated to be 0.2 m in the relevant spatial dimension (perpendicular to the parabola vertex). It must be stated that this value can only be achieved if the assumed solar field geometry is realistic.

In order to detect and compare absorber tube reflections from a series of images, while the SCE position within the image varies between consecutive frames, it is indispensable to rectify each image and create matrices (ortho images) with an aspect ratio that corresponds to actual collector aperture. Each pixel in the ortho-image matrix can

³ Camera optical axis vertical

⁴ By image processing

be assigned to a specific location in the ideal concentrator geometry. Same locations of the mirror surface appear at identical positions in the ortho-image matrix, so that subsequent results of the image processing (detection of the absorber tube reflection) can be combined in a single matrix. The tube reflection pattern is also exploited to calculate the orientation of the optical axis of each SCE.

As mentioned above, the QFly_{SURVEY} flight route design does not permit the simultaneous and independent measurement SD_X , ΔX_{Abs} and ΔZ_{Abs} . Hence, only the effective slope deviation SD_{Xeff} can be derived for the mirror shape. The basic calculation follows the procedure described in (Ulmer, Heinz et al. 2009).

A major advantage of the large field of view of the QFly_{SURVEY} data acquisition is the possibility to derive effective tracking deviation ($\Delta\theta$) for each SCE of the solar field, which so far has not been accessible at this scope and spatial resolution. If the orientation of the optical axis of each SCE is known, the inter-SCE alignment and torsion of the entire SCA can be checked, as well as inclinometer off-sets of the solar field data acquisition system. These results enable general performance analysis and optimization of the tracking system which is by far the easiest way to boost the solar field performance.

The results presented here are based on an approach from former investigations by NREL on characteristic pattern or "fingerprints" of the absorber tube reflection caused by concentrator imperfections (Jorgensen, Burkholder et al. 2009). This approach is implemented and enhanced by a robust method to match simulated and measured pattern. The first step is the creation of simulated pattern based on the camera position, and averaged measured SD_X , and HTF temperature dependent ΔZ_{Abs} values. The second step is the creation of measured pattern from tube reflex images and the comparison with simulated pattern in order to derive $\Delta\theta$.

Measurement Accuracy

The measurement accuracy of QFly_{SURVEY} has been validated within the context of the measurement campaign by comparing QFly_{SURVEY} with results obtained from four SCAs, which have been measured with already validated benchmark approaches. The overall accuracy is expressed by the root mean square of differences between QFly_{SURVEY}- and benchmark results. The RMS value of the differences between airborne collected tracking angle θ (or tracking deviation $\Delta\theta$) and inclinometer benchmark data is 1.4 mrad, while expected measurement accuracy is in the range of 0.9 - 1.3 mrad. The measurements correspond remarkably well, taking into account the fact that the benchmark measurement itself reveals an uncertainty of 1.0 mrad.

The quantitative comparison of SD_{Xeff} maps from QFly_{SURVEY} and the already validated QFly_{HighRes} approach for four SCAs (corresponding to a total aperture area of $\sim 3500 \text{ m}^2$) revealed, as expected, a slight underestimation of SD_{Xeff} results of QFly_{SURVEY} due to the reduced spatial resolution and reduced number of images per SCA. However, SD_{Xeff} show very good qualitative matching, and the SD_{Xeff} RMS values match with differences between 0.1-0.4 mrad. A detailed description of the methods and validation is beyond the scope of this article and will be presented in a separate publication.

RESULTS

Field Performance

The objective of the measurement of the solar field optical performance is to get a general overview on the concentrator quality in terms of average values and distribution of effective shape and tracking deviations, as well as the identification of problematic areas with significantly reduced performance. The challenge of this evaluation is the fact that the huge amount of data does hardly permit user interaction and individual quality checks of each single result. In order to cope with artifact arising from bad data quality (e.g. few samples, error of image processing), each result is provided with several quality criteria. That way, only reliable results are used.

SD_{Xeff} results of the investigated area (Block NE & SE) show two different characteristic pattern as presented in FIGURE 2. Block NE and a part of SE show moderate slope deviations with a RMS SD_{Xeff} value in the range of 2-3 mrad. Yet, from a certain point in the solar field on, the slope deviation pattern is more pronounced, resulting in RMS SD_{Xeff} up to 4.5 mrad. The histograms presented in FIGURE 3 provide the RMS values of SD_{Xeff} of each SCA.

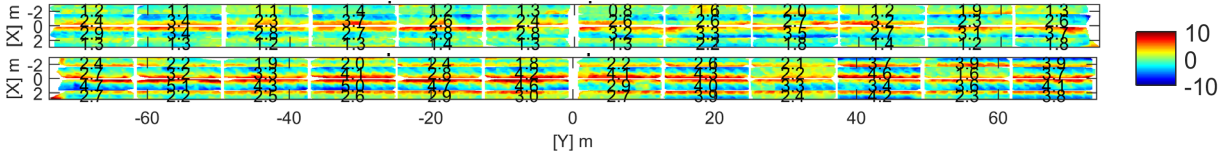


FIGURE 2. Top: Typical $SD_{X_{eff}}$ pattern of an AS3 SCA with an RMS value in the range of 2.5 mrad. Dominant features are the typical and inevitable superimposition of initial mirror shape and deformations due to gravity load.

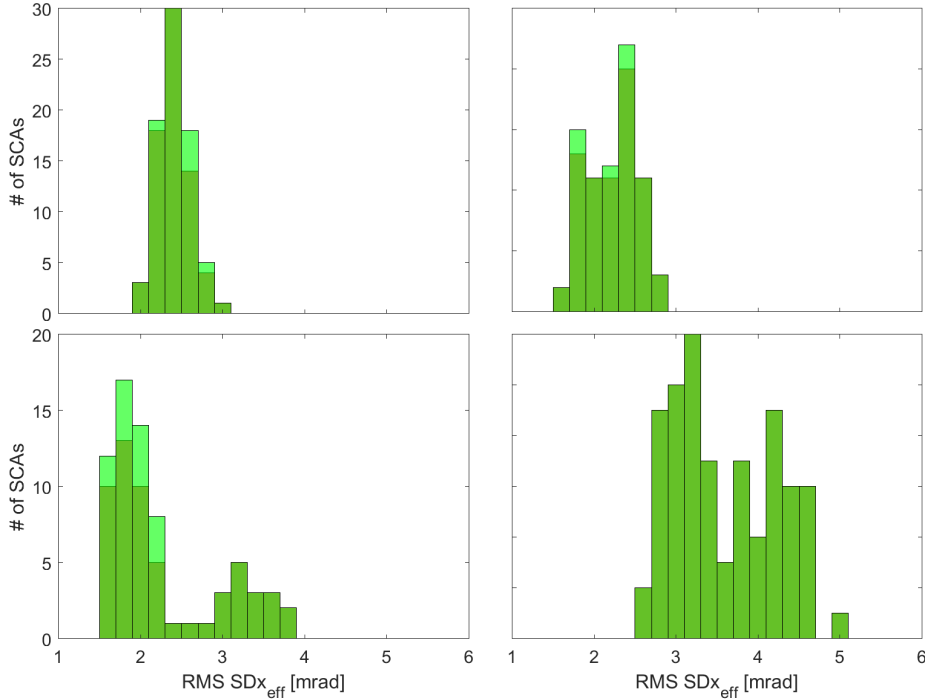


FIGURE 3. Histogram of $SD_{X_{eff}}$ pattern for Block NE north (top left), NE south (top right), SE north (bottom left), and SE south (bottom right). The light green bars refer to results with reduced reliability. While the Block NE shows mono modal slope deviation distribution, there are two types of SCAs with different optical quality present in the northern part of SE (bottom left). The southern part of SE shows consistently a comparatively low shape quality, which could explain the lower thermal performance of this block.

The difference in the northern part of the SE block results in two peaks, while the $SD_{X_{eff}}$ continues comparatively low in the southern part of SE. The reason for the sharp change is yet unclear. In the first place, $QFLY_{SURVEY}$ is used to uncover such irregularities. In order to cross-check such results and to understand the underlying causes, further measurements with $QFLY_{HighRes}$ on a random basis are required. From the current point of view it can be stated, that the observed $SD_{X_{eff}}$ pattern suggest the mirror panels and/or their interconnection with the steel structure as a cause since the mutual orientation of mirror pads and steel structure has a significant influence on the optical performance. Systematic torsion or absorber tube deviations would lead to a different characteristic $SD_{X_{eff}}$ pattern.

Concerning the quality of the individual orientation of SCEs and the tracking quality of the entire SCA, several phenomena have been observed. As the solar field was set to fix zenith orientation during the measurement ($\theta = 90^\circ$), this value was denoted as set point. Measured quantities are absolute individual orientation of each SCE, which allow comparing the orientation of the SCA as whole with the set point, as well as the comparison of the actual orientation of the SCE at the drive pylon with the value returned by the inclinometer at this particular position.

Furthermore, the alignment of SCEs within the SCA provides information about twist due to operational loads and/or the mutual alignment during the assembly of the SCA. **FIGURE 4** provides examples on observed irregularities, while **FIGURE 5** shows the distribution of statistical values for a selected part of the solar field.

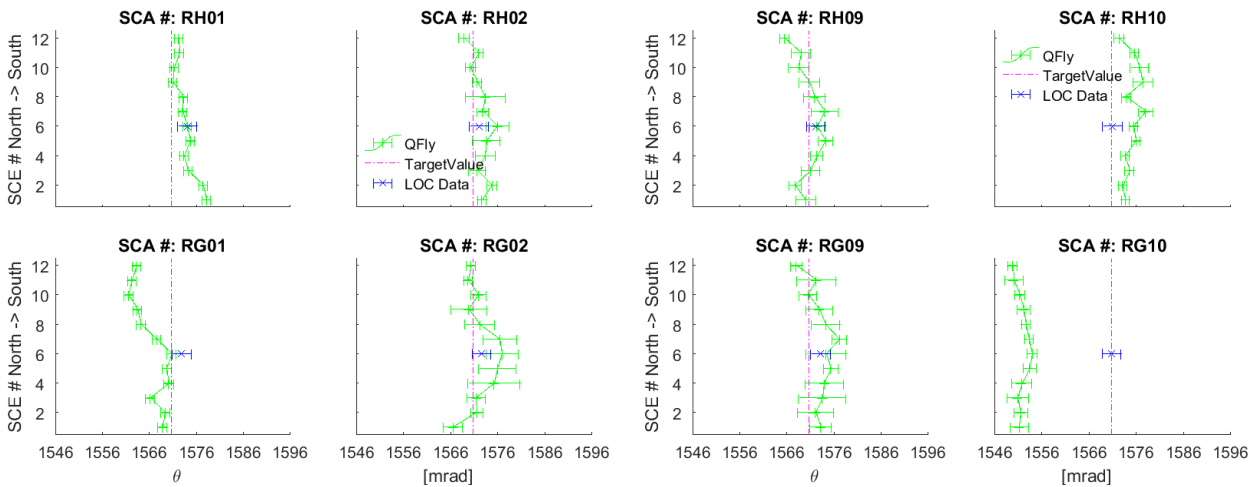


FIGURE 4. Example for possible irregularities concerning tracking and SCE alignment. The graphs display the absolute orientation measured by QFly_{SURVEY} of each individual SCE within one loop. The set point of 90° ($\cong 1570.8$ mrad) is denoted by a vertical red line (target value). The value returned by the inclinometer of the solar field control system (LOC) is marked with a blue symbol. SCA RG01 is an example with significant misalignment or torsion. Due to erroneous mounting of the inclinometer, the entire SCA RG10 shows a systematic deviation from the set-point, while there is no twist or misalignment observed within the SCA RG10 itself. For this SCA, the deviation between the actual orientation returned by QFly_{SURVEY} and the value indicated to field control system differs by 1.5°, which would affect the performance in virtual or inclinometer based tracking.

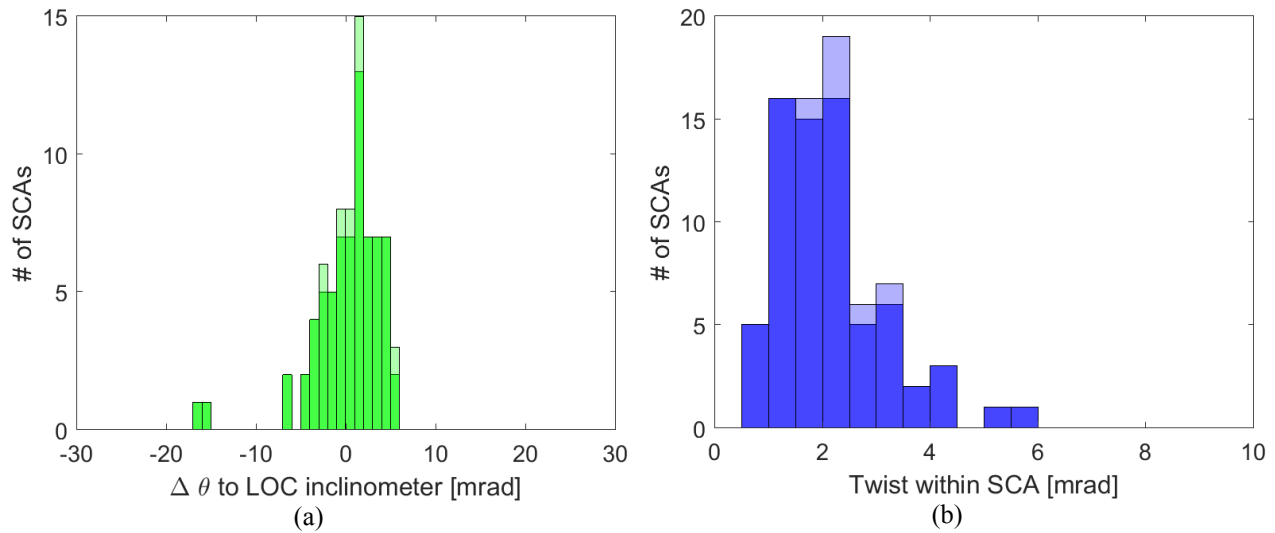


FIGURE 5. Statistical values of the orientation of SCEs and the tracking quality. (a): Sample distribution of inclinometer misalignment. In most cases, the orientation of the SCE at the drive pylon matches well with the value acquired by the solar field control system. However, in some cases, deviations in the range of 15 mrad ($\sim 1^\circ$) have been observed. (b): sample distribution of RMS value of misalignment or twist/torsion relative to drive pylon. The majority of the collectors is very well aligned, but there are some outliers which provide the potential for significant performance improvement by reduction of friction and/or retrofitting of the alignment.

Field Status

The condition of components in the solar field targets primarily mirrors and absorber tubes. The presence of intact mirrors can be checked with 100% accuracy by QFly_{SURVEY} in *offline* mode. This is achieved by a rather simple approach where the luminosity of the ortho images is checked, If a mirror panel appears in the entire image series, it is assumed that this mirror is missing. Table 1 presents the statistics of broken mirrors as detected by QFly_{SURVEY} during the campaign in 2016 Q4. Irregularities of the absorber tube, in particular broken glass envelope tubes show diverging appearance, depending on how long the unprotected selective coating has been exposed to ambient air. The coating tends to degrade with time so that for recently broken glass envelope tubes, the tube reflex is very dark even under concentrated illumination, while degraded coatings provide a very bright signal. In any case, broken glass envelope tubes are best detected when the field is in operation (*online* mode). However, the wide range of possible appearances complicates doubtless identification in the visible range. Data acquisition with an infrared camera is expected to deliver a clear signal in this case:

TABLE 1. Absolute and relative number of missing mirror panels as detected by QFly_{SURVEY}

Block	# of missing mirror panels	relative
NE North	44	~ 1.7‰
NE South	32	~ 1.2 ‰
SE North	23	< 1.0 ‰
SE South	16	< 1.0 ‰

POTENTIAL FOR OPTIMIZATION

The proper prediction of the optical performance of the entire solar field based on the geometrical measures presented here requires a holistic interface to ray-tracing software. As this interface is not yet capable to handle the huge amount of data efficiently, a rough estimation of the effect of the observed mirror shape and tracking deviations based on look-up tables and statistical considerations is presented here. That way, threshold values can be set from where corrective measures should be taken into account. The potential to improve the solar field performance is determined on the one hand by the positive impact of deviations and irregularities on the performance, and on the other hand by the financial effort for the corrective actions.

- In case of the missing mirrors, replacement can be done easily, however the observed status of the solar field is uncritical, or in other words, the replacement of broken mirrors would hardly affect the performance.
- The effect of the effective mirror slope deviation on the optical and thus thermal performance is largely affected by the increased deviations in the southern part of the solar field. The decrease in the intercept factor and such in the optical performance by the increase of the RMS $SD_{\chi_{eff}}$ from 2.5 to 4.0 mrad is in the range of 5-10%, depending on the assumptions on the sunshape and tracking accuracy of the drive system (Pottler, Ulmer et al. 2014, Figure 1 and Table 1). After a detailed measurement using the QFly_{HighRes} mode, the scope of action to improve this feature will be clearer.
- An isolated investigation of the effect of inclinometer misalignment and SCE misalignment or torsion reveals a large and cost-effective potential for optimization. An SCA in virtual track mode⁵ with a tracking offset of 15 mrad would have an intercept factor below 50%. The effect of the observed values for torsion and misalignment are less severe, but still offers the potential for optimization of individual SCAs with comparatively low effort.

CONCLUSIONS AND OUTLOOK

The first demonstration and validation of QFly_{SURVEY} in a commercial CSP plant has shown the capability of this measurement method to unveil the potential for optimization in a parabolic trough plant which already performs

⁵ Following the inclinometer and not the sun sensor.

beyond the expectations. The data acquisition could be carried out without affecting the usual plant operation. The measurement accuracy has been validated and is sufficient to doubtlessly identify typical geometric deviations.

Regions with higher $SD_{X_{eff}}$ could be identified in the SE block in accordance with the observed lower thermal performance. In these regions, the future application of the QFly_{HighRes} mode will provide more insight into the geometric characteristics. Based on that additional measurement, the identification of optimization measures will be possible.

Besides of the effective mirror slope, the tracking deviation and the twist inside a collector could be measured and striking SCAs could be identified. Causes for that behavior will be identified by the O&M team of MQS. In addition, statistics and locations of the broken mirror panels in the solar field could be derived.

The enhancement of the capabilities of the QFly measurement system is currently going on. This implies the development of a largely automated system for solar field performance ($SD_{X_{eff}}$, $\Delta\theta$) and solar field status (mirror panels, glass envelope tubes, heat loss, friction of swivel joint, cleanliness, HTF leakage) characterization. The application to heliostat fields (airborne tacking- and shape characterization) will be implemented in a future R&D project.

ACKNOWLEDGMENTS

We thank Marquesado Solar for the cooperation and access to Andasol 3 plant. The development of the QFly system is currently being supported by the DLR Technology Marketing. The results presented here are partly based on R&D activities funded by the German Federal Foreign Office (contract 3002762)

REFERENCES

1. Dinter, F. and D. M. Gonzalez (2014). "Operability, reliability and economic benefits of CSP with thermal energy storage: first year of operation of ANDASOL 3." [Energy Procedia](#) **49**: 2472-2481.
2. Grussenmeyer, P. and O. Al Khalil (2002). "Solutions for exterior orientation in photogrammetry: a review." [The photogrammetric record](#) **17**(100): 615-634.
3. Jorgensen, G., F. Burkholder, et al. (2009). Assess the Efficacy of an Aerial Distant Observer Tool Capable of Rapid Analysis of Large Sections of Collector Fields, NREL.
4. Pottler, K., S. Ulmer, et al. (2014). "Ensuring Performance by Geometric Quality Control and Specifications for Parabolic Trough Solar Fields." [Energy Procedia](#) **49**(0): 2170-2179.
5. Prah, C., B. Stanicki, et al. (2013). "Airborne shape measurement of parabolic trough collector fields." [Solar Energy](#) **91**(0): 68-78.
6. Ulmer, S., B. Heinz, et al. (2009). "Slope error measurements of parabolic troughs using the reflected image of the absorber tube." [Journal of Solar Energy Engineering](#) **131**(1): 011014.
7. Xiao, J., X. Wei, et al. (2012). "A review of available methods for surface shape measurement of solar concentrator in solar thermal power applications." [Renewable and Sustainable Energy Reviews](#) **16**(5): 2539 - 2544.